Publications

Available Online

J. Sci. Res. **16** (3), 817-834 (2024)

JOURNAL OF SCIENTIFIC RESEARCH

www.banglajol.info/index.php/JSR

Carboxymethyl Cellulose/Poly(Acrylamide-co-Vinyl Imidazole) Based Self-healing Hydrogel for Supercapacitor Applications and Moisture Determination (Part-II)

D. Dubey, S. K. Bajpai*, M. Bajpai

Polymer Research Laboratory, Department of Chemistry. Govt. Model Science College, Jabalpur (M.P.)-482001, India

Received 18 November 2023, accepted in final revised form 16 January 2024

Abstract

Physical entanglements between carboxymethyl cellulose chains and poly(acrylamide-co-vinyl imidazole) have resulted in a unique solid hydrogel electrolyte (SHE) material with highly controllable properties. The SHE showed an excellent self-healing property, as confirmed by the "LED glowing" experiment, and the 'self-healed 'material recovered 78 % of its original elongation capacity. The freshly prepared SHE, when put on the copper surface, required a detachment pressure (DP) of 864 Pa, while a fairly high DP of 8909 Pa was required after 24 h of contact. The SHE sample was highly flexible and regained its shape after knotting, folding, and twisting. The hydrogel also exhibited shape memory property. Finally, the samples SHE-I and SHE-IV (containing 0 and 4 mL glycerol per 40 mL of film forming solution) were charged using a 12-volt supercapacitor for 2 min and then employed to glow LED bulb as well as run alarm clock. It was found that sample SHE-I was able to glow the LED bulb for almost 55 min, while sample SHE-IV successfully lit the LED for almost 357 min. Similarly, a small alarm clock was run by the two SHE systems for 118 and 838 min, respectively.

Keywords: Solid hydrogel electrolyte; Adhesion; Self-healing; Capacitor.

doi: https://dx.doi.org/10.3329/jsr.v16i3.69942 J. Sci. Res. **16** (3), 817-834 (2024)

1. Introduction

In the last few years, hydrogels with self-healing properties have been a focus of attention for material scientists, probably due to a wide range of their applications in different fields like wearable, flexible devices, [1-3] electronic skin, [4,5] biomedicine, [6-8] tissue engineering, [9,10] cell therapy, wound dressing, [11,12] etc. A number of approaches have been employed to fabricate self-healing hydrogels. These include hydrogen bonding, host-guest recognition, electrostatic interactions, hydrophobic associations, metal-ligand coordination, dynamic covalent bonds, etc. [13-18].

A fairly high-water content, flexibility, and adhesiveness are the basic requirements for the use of these hydrogels in biomedical fields such as tissue engineering. On the other

* *Corresponding author*: sunil.mnlbpi@gmail.com

hand, using these hydrogels as storage energy devices requires high conductivity, flexibility, and fair mechanical strength. However, the development of a hydrogel with the above-mentioned properties still remains a challenge. The reason is that fairly high-water content usually results in a brittle polymer matrix. Similarly, a fairly high movement of polymeric segments is required for self-healing property, but this automatically reduces the mechanical strength [19,20]. Therefore, in order to have a hydrogel with all such desired properties, a proper selection of monomers and polymers is required so that the polymer formed has an appropriate combination of hydrophilicity, bonding strength, presence of protonated /deprotonated groups, and mutual entanglements of polymer chains.

In this work, a sincere attempt is made to fabricate a physically crosslinked hydrogel with electrical conductivity, self-healing, anti-freezing, and adhesiveness. The solid hydrogel electrolyte (SHE) is made from a polysaccharide carboxymethyl cellulose (CMC) and copolymer poly (acrylamide-co-vinyl imidazole(AAm-co-VI). The rationale for the selection of these constituents is as follows: (i) CMC is a highly water-soluble polymer with hydrophilic groups that have a fair tendency to interact with water molecules. (ii) the copolymer poly(AAm-co-VI) contains amide and imidazole groups, respectively, that can produce intermolecular H-bonding interactions to provide a stable polymer matrix with proper water holding capacity and fair tendency of self-healing. (iii) Finally, mutual entanglements between CMC polymeric chains and linear copolymer poly (AAm-co-VI) segments provide additional stability to the polymer matrix.

However, the recent past has witnessed tremendous research work on self-healing hydrogels, as mentioned above. However, most of the studies have focused mainly on self-healing properties. Here, in this work, apart from the excellent self-healing property, the proposed hydrogel also possesses shape memory property, strong adhesion to metallic surfaces, and remarkable toughness; all these features make it a potential candidate for multiple applications. In addition, this hydrogel has a unique feature: its remarkable water absorption property in highly acidic and alkaline media (reported in a separate communication as Part-I that is under review), which makes it a suitable candidate for gastric drug delivery. In this way, the proposed hydrogel system is a combination of a number of significant properties that make it a polymeric material with a wide range of applications.

2. Experimental

2.1. *Materials*

Vinyl monomers, Acrylamide (AAm), and Vinyl imidazole (VI) were purchased from Hi-Media Chemicals, Mumbai, India. Monomer AAm was re-crystallized in methanol to remove the inhibitor. Carboxymethyl cellulose (CMC), initiator potassium persulfate (KPS), and other salts were also purchased from Hi Media Chemicals and used as received. The double distilled water was used throughout the investigations.

2.2. *Preparation of solid hydrogel electrolyte (SHE)*

The SHE was prepared by carrying out free radical co-polymerization of monomer AAm and VI in the presence of dissolved CMC. A pre-determined quantity of monomers AAm and VI was mixed into a definite volume of CMC solution, followed by the addition of glycerol (if required) and initiator KPS. The pre-polymerization mixture was poured into plastic rectangular molds and kept in an electric oven (Tempstar, India) at 40 ^{o}C for 1 h. Finally, the films were taken out carefully and placed in Polyethylene bags for further use. In all, four samples were prepared with different compositions, as given in Table 1.

Table 1. Composition of various solid hydrogel electrolytes synthesized at 40 °C.

Sample code	Composition of SHE samples*			
	CMC (g)	AAm (g)	VI (mL)	Glycerol (mL)
SHE-I	0.64	6.0	3.0	-
SHE-II	0.64	6.0	3.0	2.0
SHE-III	0.64	6.0	3.0	3.0
SHE-IV	0.64	6.0	3.0	4.0

2.3. *Rheological analysis of sample SHE*

The Rheometer (HAAKE MARS) was used to test the rheological behavior of sample SHE-I. The storage modulus (G') and loss modulus (G") were determined under two sets of experiments: (i) shear frequency was changed from 0.1 to 100 Hz (0.628 rad/s to 628 rad/s) with strain kept constant at 1 %, and (ii) strain sweep varying from 1 to 100 % with frequency fixed at 6.28 rad/s. All the experiments were performed at 25 °C.

2.4. *Tensile tests*

The tensile properties of hydrogel samples were determined using a commercial tensile testing machine (Instron 3343) with a stretch rate of 50 mm/min at 25 °C. The samples were prepared by cutting the hydrogel sheet in a dumbbell shape, having 12 mm and 2 mm as initial gauge length and width, respectively. The Young modulus was determined using the initial slope of strain versus strain curve when the strain was less than 10 %. All the experiments were carried out at 25 °C.

2.5. *Adhesion capacity of SHE*

For measurement of the adhesion capacity of hydrogel over different surfaces, hydrogel sample SHE-I was prepared in a cylindrical shape, and one end was stuck on the middle of the surface of different metallic/nonmetallic objects for a period of 10 min. Now, various weights in increasing order of magnitude were placed on objects till the hydrogel surface was totally detached from the object. In the next set of experiments, the freshly prepared hydrogel was left stuck for a period of 24 h and then detached from the surface following

the same procedure. The Detachment pressure (DP) was calculated using the following expression:

$$DP = \frac{F}{A}\ Pa \quad (1)$$

Where F= Force required to detach the surface (N)
A = Area of the surface of an object (m^2)

2.6. *Elongation properties of SHE films*

The solid hydrogel electrolyte film samples SHE-I, II, III, and IV were investigated for their percent elongation capacity (PEC) at 25 °C. The tests were performed in two sets. In the first set of experiments, the SHE film samples were used as such without any further treatment. In the second set of experiments, all the film samples were conditioned by suspending them for 24 h in the humid environment created in a plastic jar filled with water (100 % humidity). Their percent elongation capacity (PEC) was measured by using an Instron Universal Testing Instrument\(Model 1011). The initial grip separation and mechanical crosshead speed were set at 40 and 200 mm per min, respectively. The PEC was calculated using the following expression:

$$PEC = \left(\frac{L_i - L_e}{L_i}\right) X\ 100 \quad (2)$$

Where, L_i refers to the initial length of the test sample and L_e is the length of the elongated sample before break. All the determinations were made in triplicate.

2.7. *Fabrication of SHE rechargeable supercapacitor*

The SHE-based Supercapacitor was fabricated as described as follows: A completely used cell (initial voltage 1.5 V, Eveready Industries Limited, India) was broken gently to take out the Carbon electrode. This electrode was placed at the corner of a hydrogel sheet, having a dimension of 18 poly × 5 cm. Now, this SHE sheet was placed on an aluminum foil (RSF Hytek Private Limited, India), with a dimension of 20 × 5 cm, and rolled over to give a cylindrical shape.

2.8. *Setup for charging-discharging process*

To prove the electrochemical performance of the Supercapacitor SHE-I and SHE-IV(without and with glycerol), each was connected in series with a chargeable battery (Loom Solar, Model CAML1212, India) and allowed to be charged for a period of two min and the voltage acquired was recorded in a multi meter (Unit, India, model-DT830D). After charging the hydrogel capacitor, it was allowed to get discharged through the light-emitting diode (LED) so as to establish evidence for practical applications.

2.9. *Fabrication of GAHM (gravimetric air humidity monitor (GAHM))*

In order to fabricate a gravimetric air humidity monitor (GAHM), a highly porous sample SHE-I was prepared by addition of 5 g of $CaCO_3$ in 30 mL of polymerization mixture under vigorous stirring and ultrasonication to ensure complete mixing of $CaCO_3$ particles within the pre-polymerization mixture, now, 10 mL of this reaction mixture was taken in a Test tube and kept in electric oven at 45 °C for a period of 1h. The test tube was broken in water, and the gel was taken out and cut into thin slices with the help of a sharp blade. Now, the thin slice was placed in 250 mL of 2M HCl solution for a period of 6 h. The porous sample, thus obtained, was vacuum dried, and a small hole was made at its center with the help of a drawing pin so that the disc could be hung during air during humidity measurements.

2.10. *Calibration plot for humidity measurements*

The mass of the disc was determined using an electronic balance (Denver). Now various saturated salt solutions, (LiCl, CH_3COOK, $MgCl_2$, $Mg(NO_3)_2$, NH_4NO_3, NaCl, $(NH_4)_2 SO_4$, KNO_3 and H_2O with their respective RH of 11, 22, 32, 51, 60, 75, 81, 92 and 100, were prepared in 100 mL plastic bottles and GAHM was suspended inside the air-tight bottles using a copper loop and kept in a thermostat at 30 ^oC for a period of 600 s. Now, the GAHM was taken out from each bottle, and its mass was determined using an electronic balance (Kern, PFB 120-3). The equilibrium moisture uptake (EMU) in mg/g was determined as:

$$\text{EMU} = \text{Moisture uptake (mg)} / \text{weight of GAHM (g)} \quad (3)$$

A calibration curve was plotted between % RH and corresponding EMU values.

2.11. *Determination of unknown air humidity*

The laboratory -made GAHM, shown in Fig. 9c, was placed in open air for a period of 10 min, and its mass was recorded by electronic balance and transformed into % RH using the calibration curve.

3. Results and Discussion

3.1. *Preparation of SHE*

In this work, solid hydrogel electrolyte (SHE) was prepared by carrying out free radical-initiated polymerization of monomers AAm and VI in the presence of dissolved CMC in aqueous medium. As no crosslinker has been used in the reaction mixture, the linear chains of copolymer poly(AAm-co-VI) and carboxymethyl cellulose (CMC) are entangled with each other to form a closed matrix. The matrix, thus formed, is additionally stabilized due to hydrogen bonding interactions between carboxymethyl groups of CMC, imidazole groups of VI, and amide group of AAm. These H-bonding interactions play a major role in

empowering SHE with self–healing and adhesion properties. All such possible H-bonding interactions and mutual entanglements are illustrated in Fig. 1**.**

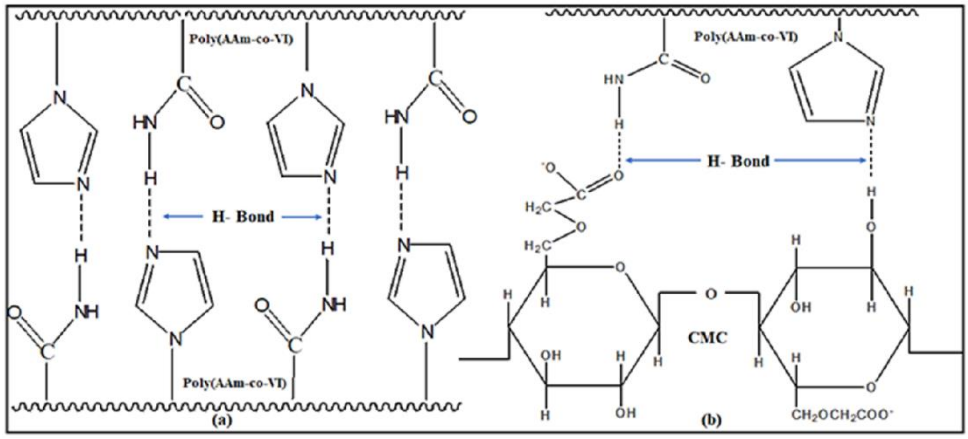

Fig. 1. Possible H-bonding interactions within the hydrogel matrix.

3.2. *Rheological behavior and Tensile analysis of SHE-I*

The results of dynamic rheological tests for the sample SHE-I are shown in Fig. 2. It is clear from Fig. 2a that the value of storage modulus G' is much higher than the value of loss modulus G" in the frequency range studied. In addition, these values remain almost constant throughout the applied frequency range. This suggests that the hydrogel has a fairly stable structure and remains almost unaffected by varying frequency. The fair stability of the structure indicates that hydrogen bonds present within the polymer network (as depicted in Fig. 1 also) are strong enough to resist the applied frequency sweep. Finally, mutual entanglements of polymeric chains, coupled with strong H-bonding interactions, render fair stability to the sample SHE-I. Moreover, the intact structure of the hydrogel was further confirmed when the strain was varied up to 100 %, keeping the frequency at 6.28 rad/s (please see Fig. 2b). Here, the values of G' and G" remain almost unaltered. Almost similar results have been reported by Fu *et al.* [21], who prepared Fe(III)-coordinated carboxymethyl chitosan/poly(acrylic acid) hydrogels which retained their G' and G" values almost constant on applying frequency and strain sweep. However, there have been several studies that report the decline in G' and G" values on applying strain. For example, Yan *et al.* [22] fabricated poly(acrylamide)/polyethyleneimine hydrogel in glycerol-$CaCl_2$ water medium and found that G' and G" values remained constant up to the 30 % strain but later on decreased with further applied strain due to rupture of hydrogen bonds

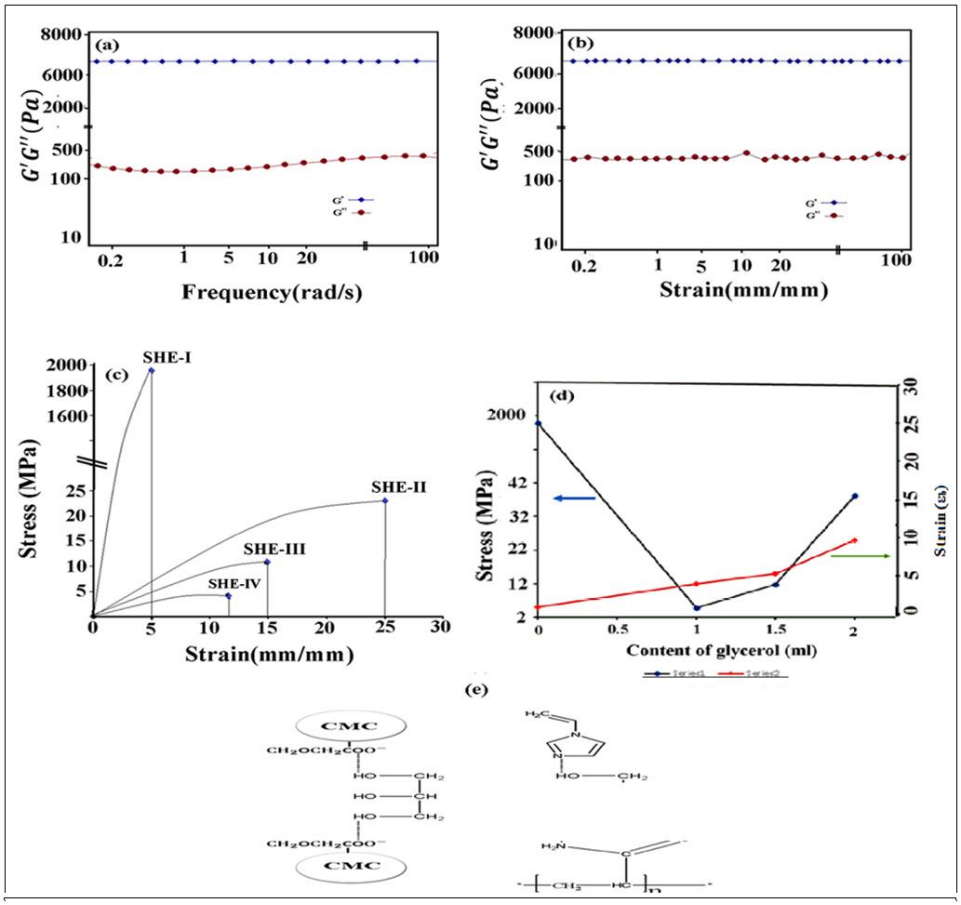

Fig 2. Dynamic rheological behaviors of the sample SHE-I. (a) Frequency sweeps, (b) strain sweep, (c)stress-strain curves for the samples, (d) corresponding mechanical parameters, (e) Possible H-bonding interaction between glycerol molecules and constituents.

The results of stress-strain experiments for the samples SHE-I(without glycerol), SHE-II, SHE-III, and SHE-IV(congaing different amounts of glycerol) are given in Fig. 2c. The variations in respective tensile breaking stress (σ_b) and breaking strain (ε_b) are also shown in Fig. 2d. It can be observed that the sample SHE-I exhibits the highest value of Tensile strength (1958 MPa) and minimum Elongation at break (5 mm/mm). This is attributable to the fact that there are excessive H-bonding interactions between various functional groups of constituents, as illustrated in Fig. 1. These interactions do not allow the hydrogel to elongate much, and high stress is required before the hydrogel breaks. It is also noticed that a drastic decrease in tensile strength is observed for the sample SHE-II (containing 2.0 mL of glycerol) as compared to sample SHE-I. The observed decrease is attributable to the fact that glycerol molecules occupy the space and reduce the intra-molecular affinity of CMC chains by forming H-bonds. Hence, hydrogel becomes less dense and facilitates the mobility of polymeric segments [23], thus causing an increase in Elongation values at the

break. Similar results have been reported elsewhere [24,25]. However, let's compare the results obtained for the samples SHE-II, SHE-III and SHE-IV (containing 2, 3, and 4 mL of glycerol, respectively). It can be noticed that there is a gradual increase in the tensile at break as well as Elongation at break for all three samples. It may be due to the fact that glycerol molecules form much stronger H-bonds with N and $–NH_2$ groups of imidazole and acrylamide units, thus enhancing the strength of the polymer. In addition, the presence of glycerol molecules between polymeric chains also causes an increase in the mobility of the polymeric segments, thus enhancing Elongation at the break. The possible interaction of glycerol molecules with polymer constituents is depicted in Fig. 2e.

3.3. *Adhesiveness and flexibility of SHE*

The SHE, under investigation, demonstrated very strong adhesive properties that varied from substrate to substrate. The adhesion capacity was measured in terms of Detachment Pressure (DP), which may be defined as the pressure required to detach the hydrogel from the surface of any object. The hydrogel sample SHE-I was placed on the surface of various substrates (Fig. 3a) and its DP was determined. The results, as shown in the bar diagram (Fig. 3b), indicate that values of DP increased in the following order: Glass <Bronze< Steel < Wood< Copper, thus revealing that hydrogel had a maximum DP of 8990 Pa on the Copper surface, while a minimum of 249 Pa for glass surface. The highest DP of hydrogel for copper surface may simply be attributed to the non-covalent complexation of copper atoms with (i) lone pair of N atoms of imidazole group, (ii) N atom of acrylamide, and (iii) O atoms of CMC chains. Similar interactions have also been reported previously [26]. These interactions are shown in Fig. 3c. It is also noteworthy that cellulose has the second highest DP value, probably due to the presence of a large number of hydroxyl groups in cellulose chains that bind strongly with polar groups present on the surface of sample SHE-I. We also determined the DP of the fresh samples, which was quite low (shown by green bars in Fig. 3b) when compared to the samples when dried for 24 h.

The use of hydrogel electrolytes in wearable electronics requires a fair degree of flexibility so that, in case the hydrogel is bent or twisted during the use of a smart fabric, it does not break. The flexibility of the sample SHE-I was tested by taking a straight piece of hydrogel. The strip was knotted, folded, and twisted, as shown in Fig. 6d. It was observed that there were no cracks or any sign of damage to the hydrogel. The hydrogel regained its original straight geometry when stress was withdrawn. It is also worth mentioning that there was no appreciable change in the electrical conductivity of the sample when different shapes. It was around 4.8 $x10^{-5}$ S/cm.

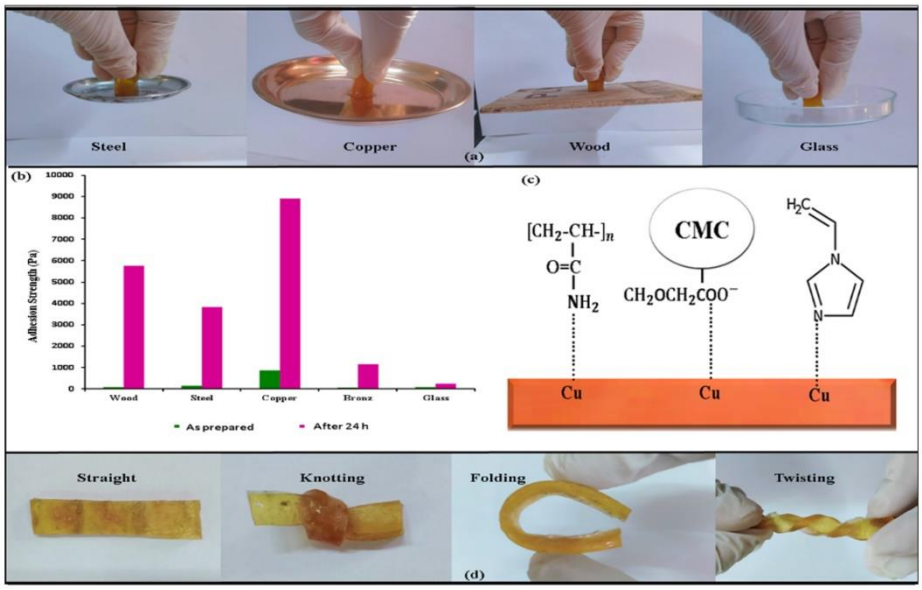

Fig. 3. (a) Freshly prepared samples were put on various surfaces, (b) Detachment Pressure of hydrogel sample SHE-I on various surfaces under different experimental conditions, (c) Metal complexation between polymeric constituents and copper atoms on the metal surface, (d) Flexibility test for the hydrogel sample SHE-I by twisting, knotting and folding the sample.

3.4. *Elongation and toughness of SHE*

The use of hydrogel electrolytes in various biomedical and smart fabric applications requires a high degree of stretchability, which the addition of a suitable plasticizer in the pre-polymerization mixture can achieve. The stretchability of the polymer can be estimated on the basis of its elongation capacity. A representative hydrogel sample SHE-I, conditioned in water vapors for a period of 24 h, was elongated to various degrees till there were signs of its rupture, as depicted in Figs. 4a-d. The strip was stretched to a maximum of almost 300 percent (see Fig. 7d) when it began to break.

In all, the percent elongation capacity (PEC) was also tested for all the samples, namely SHE-I, -II, -III, and –IV, under two different experimental conditions: (i) The freshly prepared samples SHE-I, II, III, and IV, were subjected to external stress for Elongation and (ii) these samples were placed in moist environment for 24 h followed by their elongation test. The results are shown as a bar diagram in Fig. 4e. It can be seen that in the case of 24 h dried hydrogels, the sample SHE-I (with no glycerol) showed a minimum elongation of 15 percent only. However, for other samples, namely SHE-II, III, and IV, PEC increased from 298 to 600 % as the glycerol content (per 20 mL of film-forming solution) increased from 1 to 2 mL. This may simply be attributed to the fact that glycerol molecules occupy space between the polymeric chains and thus weaken the strong H-bonding interactions among them. This ultimately reduces the firmness of polymeric chains, and they become more mobile [27]. Similar types of results have also been reported previously [28,29].

The results of percent elongation for 24 h conditioned film samples were quite different and interesting. Sample-I, with no glycerol, showed 15 % elongation when dried for 24 h, and 328 percent when conditioned in water vapors for 24 h. This is probably attributable to the fact that water molecules act as plasticizers and occupy the space in between the polymeric chains. This reduces the stiffness of the film, and the film becomes more flexible. Similarly, the sample SHE-II, containing 1 mL of glycerol and conditioned for 24 h in water vapor, shows a higher PEC of 757, probably due to the combined action of water molecules and glycerol, both of which act as plasticizers. However, the samples SHE-III and IV, containing 1.5 and 2 mL of glycerol and conditioned for 24 h in water vapor, show a reverse trend and exhibit 411 and 327 percent elongation, respectively. The observed decrease may be due to the fact that the presence of excess water vapor molecules weakens the H-bonding interactions to such a great extent that the structural integrity of these films becomes less, and therefore, they are unable to withstand the external stress. Therefore, it may be concluded that the PEC of sample SHE-II, which contains 1 mL of glycerol per 20 mL of film-forming solution, exhibits maximum Elongation.

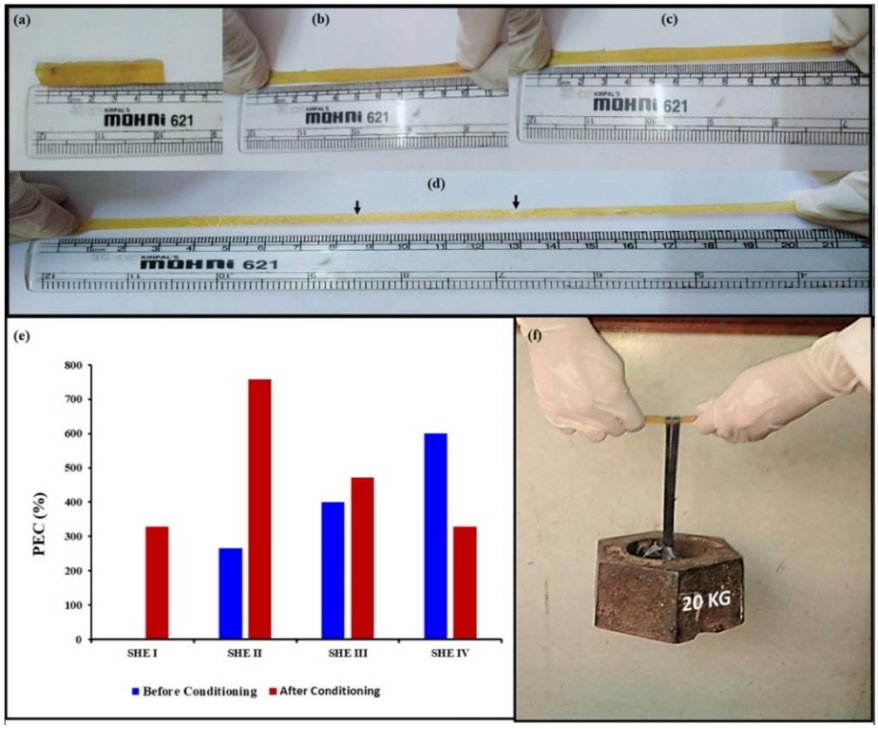

Fig. 4. (a)-(d) A piece of hydrogel sample showing its stretching at various levels, (e) Bar diagram showing PEC of various samples under different conditions, (f) 15 days-dried sample SHE-I holding a weight of 20 Kg.

Finally, the same sample SHE-I was allowed to dry for a period of 15 days, and it turned into a solid cylindrical bar with a high degree of toughness. Now, a small piece of sample

was held at its two ends, and a weight of 20 Kg was suspended in its middle, as shown in Fig. 4f.

3.5. *Shape memory property*

In order to study the shape memory property of the solid hydrogel electrolyte, a strip of freshly prepared hydrogel sample SHE-I was taken (Fig. 5a). Now, one end was held tightly, and the other one was twisted to give a spiral shape (Fig. 5b). Now the spiral strip was placed in 1 % (w/v) aqueous solution of $FeCl_3$ for a period of 1 h, which was enough to render a permanent spiral shape to the strip (Fig. 5c). The spiral-shaped strip was immersed in a 3 % ethylene diamine tetraacetic acid (EDTA) solution. The strip regained its original linear shape within a period of 1 h (Fig. 5d). The restoring of the original linear shape of the hydrogel strip in EDTA solution may be explained as follows: When the freshly prepared hydrogel strip, in spiral shape, is immersed in aqueous solution of $FeCl_3$, the imidazole groups of copolymer chains are coordinated with Fe(III) ions through their nitrogen atoms and this coordination results in a crosslinked matrix. In addition, CMC also possesses a tendency to combine with Fe(III) ions to form a crosslinked structure. Therefore, the spiral hydrogel strip acquires a fixed shape. Now, upon immersing the strip in an EDTA solution, the Fe(III) ions prefer to bind with EDTA molecules present in the external medium phase. Therefore, the iron-crosslinked spiral hydrogel strip loses its structural integrity and acquires its original linear shape.

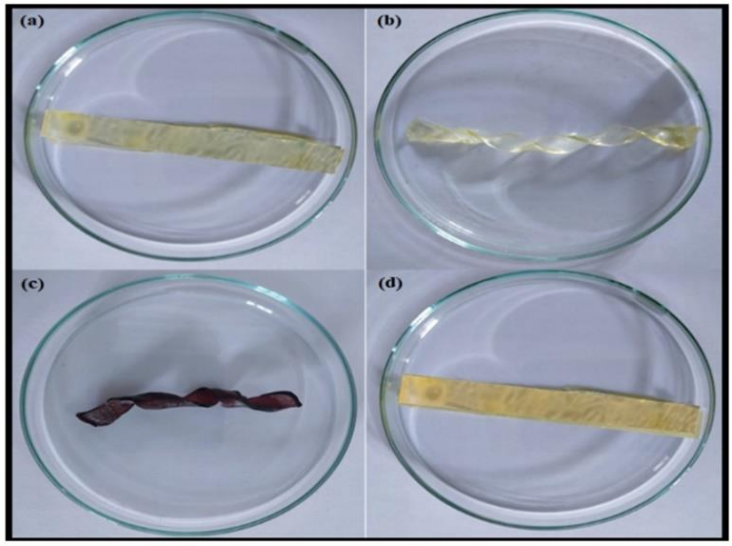

Fig. 5. (a) hydrogel strip of sample SHE-I, (b) the strip was molded into a spiral shape, (c) now put in 1% $FeCl_3$ solution for fixing, and (d) the fixed spiral strip was put in EDTA solution to regain its original linear shape.

3.6. *SHE as conducting medium to fabricate a Supercapacitor*

In the last few years, electrolytes containing hydrogels have emerged as a promising material to be employed as energy storage devices [30]. For example, Badawi *et al*. [31] have recently reported a 3-D hydrogel electrolyte composed of sodium alginate and poly (3,4-ethylenedioxythiophene)/poly(styrene sulfonate) for super capacitor applications. Similarly, Xu and co-workers have reported that capacitance of hydrogel electrolyte can be improved by pre-depositing a zwitterionic 3,4-ethylene dioxythiophene on graphene film electrode [32]. Recently, some review articles on the performance of hydrogel electrolytes as capacitors are also available in the literature [33]. In order to test the performance of SHE as a supercapacitor and to see the influence of the presence of glycerol in the hydrogel on its supercapacitor performance, samples SHE-I and SHE-IV were selected. The two SHE samples were used to fabricate batteries and were further charged using a 12-volt Supercapacitor for a period of 1 min. (as described in the section' Experimental').

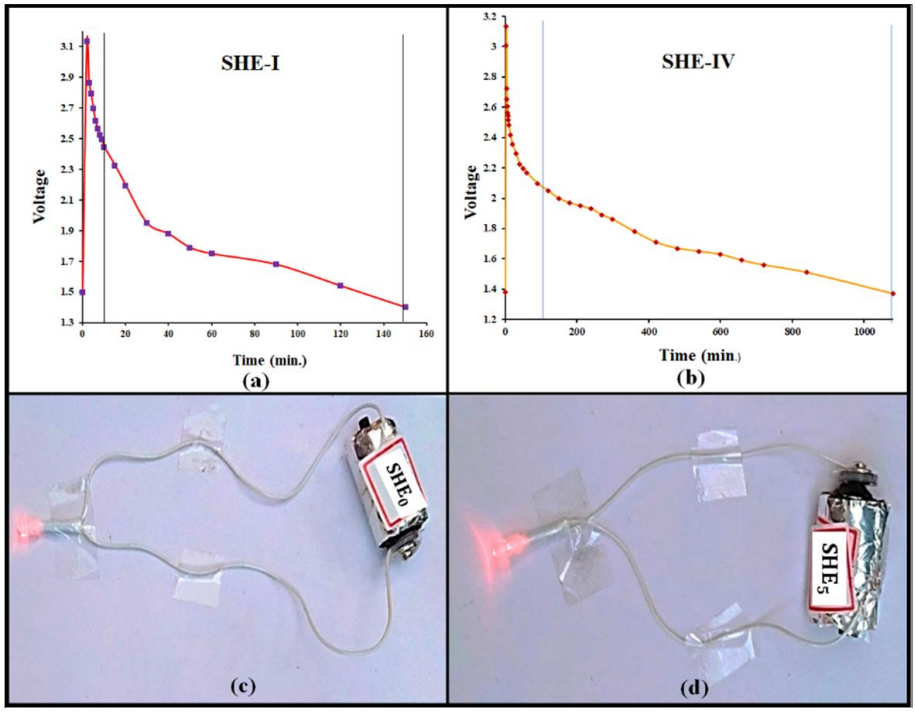

Fig. 6. Charging-discharging for the sample (a) SHE-I and (b) SHE-IV; LED glowing using the sample (c) SHE-I and (d) SHE-IV.

The results of the charging-discharging of SHE-I are shown in Fig. 6a. It was noted that the initial voltage possessed by the hydrogel supercapacitor SHE-I was around 1.48 volts. However, when this was charged with an external 12-volt supercapacitor for 2 min, it attained an optimum value of 3.14 volt. Now, the (SHE-I) began to discharge and attained

a value of 2.45 volt in 8 min. Later on, it took almost 140 min more to reach the initial value of 1.45 volts. In this way, the overall discharging can be divided into two zones: fast discharging and slow discharging, both separated by a vertical line in the above profile. The overall conclusion drawn is that (i) it took almost 3 min to charge the SHE-I from 1.45 to 3.14 volts, (ii) it discharged at a faster average rate of 0.086 volts per min. to achieve a voltage of 2.45 in 10 min, and (iii) it discharged slowly from 2.45 to 1.45 volt in next 140 min. Similarly, the charging-discharging profile of Supercapacitor SHE-IV, shown in Fig. 6b, reveals some interesting results, quite different from those we discussed for sample SHE-I. The Supercapacitor SHE-IV possessed an initial voltage of 1.38 V and took 2 min to reach a value of 3.01 volts. Now, when allowed to discharge, it took 13 min to reach a potential of 2.42 volts, thus showing a rapid discharge at an average rate of 0.06 volts per min, and finally, it took around 1065 min to discharge further to attain the initial voltage of 1.38 volt, thus showing a slow discharge extended over a longer period as compared to the SHE-I with no glycerol. The observed difference in the discharging behavior of the two SHE systems is attributable to the presence of glycerol, which keeps the internal texture more flexible and moist, thus providing a better medium for the migration of charged species.

Finally, we also employed these two samples to glow LED bulbs, as shown in Fig. 6c-d, respectively. It was found that sample SHE-I was able to glow the LED bulb for almost 55 min, while sample SHE-IV successfully lit the LED for almost 357 min. Finally, a small alarm clock was run by the two SHE systems for 118 and 838 min, respectively. This indicates that the presence of glycerol in the SHE system enhances its performance multiple times.

3.7. *Anti-freezing behavior of SHE*

As discussed above, sample SHE-I exhibits conducting behavior due to the presence of free-charged species; therefore, the hydrogel has great potential to be used in wearable smart electronics. However, in cold places, where the temperature may drop to 0 ^{o}C, the hydrogel supercapacitor may freeze and stop to function. The well-known phenomenon of freezing point depression due to the addition of an appropriate salt has been exploited recently to lower the freezing point of a hydrogel system. We added $ZnCl_2$ and glycerol to induce anti-freezing properties in the hydrogel. The anti-freezing action of samples SHE-I, SHE-IV (containing glycerol), and SHE-V (containing $ZnCl_2$) is shown in Fig. 7.

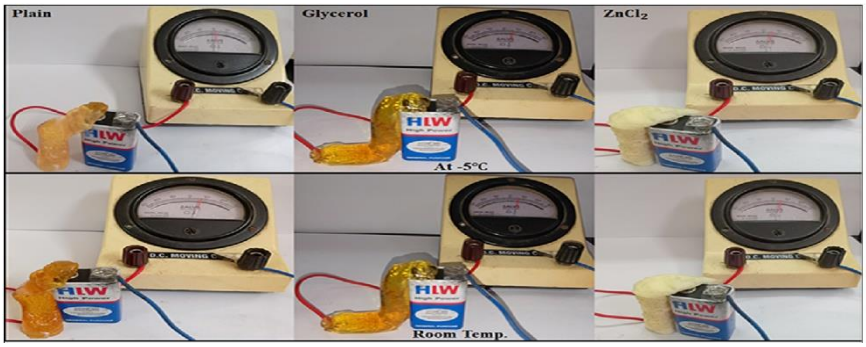

Fig.7. Anti-freezing action of samples SHE-I, SHE-IV and SHE-V at -5 and 25ºC.

It can be seen that at 25 °C, all three samples, namely SHE-I, SHE-IV, and SHE-V, show a deflection in the galvanometer when connected to a supercapacitor, thus indicating their conducting behavior. However, after putting them in a sink at -5 °C for 24 h, the sample SHE-I did not show any deflection in the galvanometer, thus indicating the presence of ice within the polymer, which stopped its function as a conductor. However, the other two samples, SHE-IV and SHE-V, showed deflection in the galvanometer as there were no traces of ice within the polymer matrix. The anti-freezing action of glycerol is well reported [34,35], and its presence prevented the aggregation of ice crystals. Moreover, the freezing point depression of the hydrogel medium in the sample SHE-V also prevented it from ice formation and aggregation.

3.8. *Fabrication of GAHM*

In the present study, sample SHE-I was made highly porous using sucrose as a pore-generating agent, as discussed in the section 'Experimental.' The addition of salt in the polymerization mixture, followed by the leaching out of the added salt from the resulting hydrogel via equilibration in the refreshing solvent, is an interesting approach to preparing porous hydrogel. However, this method is not appropriate for preparing a porous matrix with interconnected pores. Therefore, in this work, CO_2 was used as a porogen. When finely ground $CaCO_3$ powder-loaded hydrogel sample is immersed in 2M HCl solution, HCl enters into the hydrogel network and reacts with $CaCO_3$ to produce CO_2 gas, which manages to escape out through the uncross-linked polymer matrix, rendering the hydrogel a porous structure with interconnected pores. However, some CO_2 might not be able to come out of the gel. Therefore, when the gel is further placed in a vacuum desiccator, a highly porous matrix with inter-connected open pores is formed.

As mentioned above, the hydrogel synthesized was intended to be highly porous so that it could absorb moisture at an appreciably faster rate. The sample was analyzed for SEM to confirm the formation of a porous hydrogel. The images were recoded with 3, 10, and 30 thousand times magnifications as shown in Figs. 8a-c, respectively.

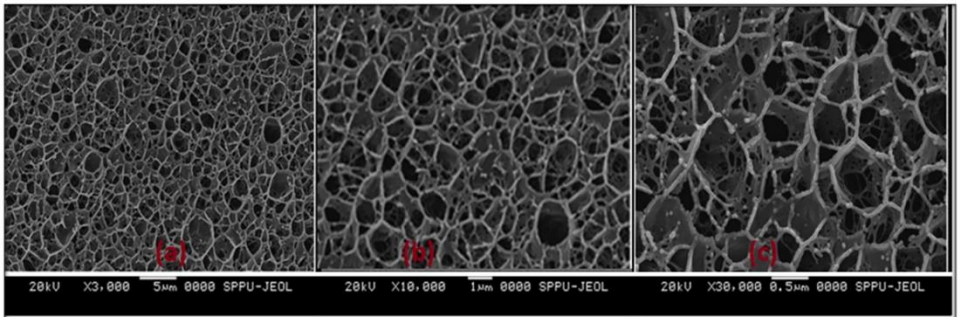

Fig. 8. Scanning electron microscopy(SEM) images of the sample imaged with (a) 3000,(b)10000, and (c) 30000 X magnifications.

It can be seen clearly that the sample was highly porous in nature and thus could probably used to absorb moisture present in the air.

3.9. *SHE as gravimetric air humidity monitor (GAHM)*

Recently, there have been several reports which describe the use of hydrogels in humidity sensing [36]. They function on the basis of the measurement of change in the electrical conductivity of the hydrogel associated with a change in its moisture uptake when exposed to an environment of varying humidity. There are basically three types: capacitive, resistive, and thermal. The major problem with them is that they require electronic circuits with equipment to measure resistance to fair accuracy. In this work, we have attempted to develop a highly porous sample SHE-I as a humidity sensor, which functions by undergoing a mass change as compared to its dry mass when exposed to a humid environment (Fig. 9a).

The results of % RH versus equilibrium moisture uptake (EMU) (mg/g) are shown in Fig. 9b. It was found that as the % RH increased, EMU values also increased in an almost linear way. However, the moisture gain by hydrophilic substrates is usually governed by a sigmoidal curve and is best interpreted in terms of the GAB model. This is due to the fact that when % RH is low, moisture is absorbed on the surface and attains equilibrium. However, at higher RH, water vapors also invade the bulk of the substrate, and a high moisture uptake is observed. The observed linear plot in the present work was due to the presence of interconnected pores within the polymer matrix, which offered a great opportunity for the invading water vapor molecules not only to get absorbed on the surface but also to enter into the bulk via an interconnected porous structure. As a result, moisture uptake of GAHM increased almost linearly with the % RH of the surrounding environment. The value of R^2 was fairly high.

The response time of GAHM was also determined by blowing hot air on it for 600 s, followed by its mass measurement and then its immediate transfer into a 75 % RH chamber for the next 600 s. As shown in Fig. 9c, a number of such drying-moisturizing cycles were repeated without any structural deformation in the hydrogel matrix. In addition, the EMU values obtained in each cycle were almost the same, thus establishing the reproducibility of the device.

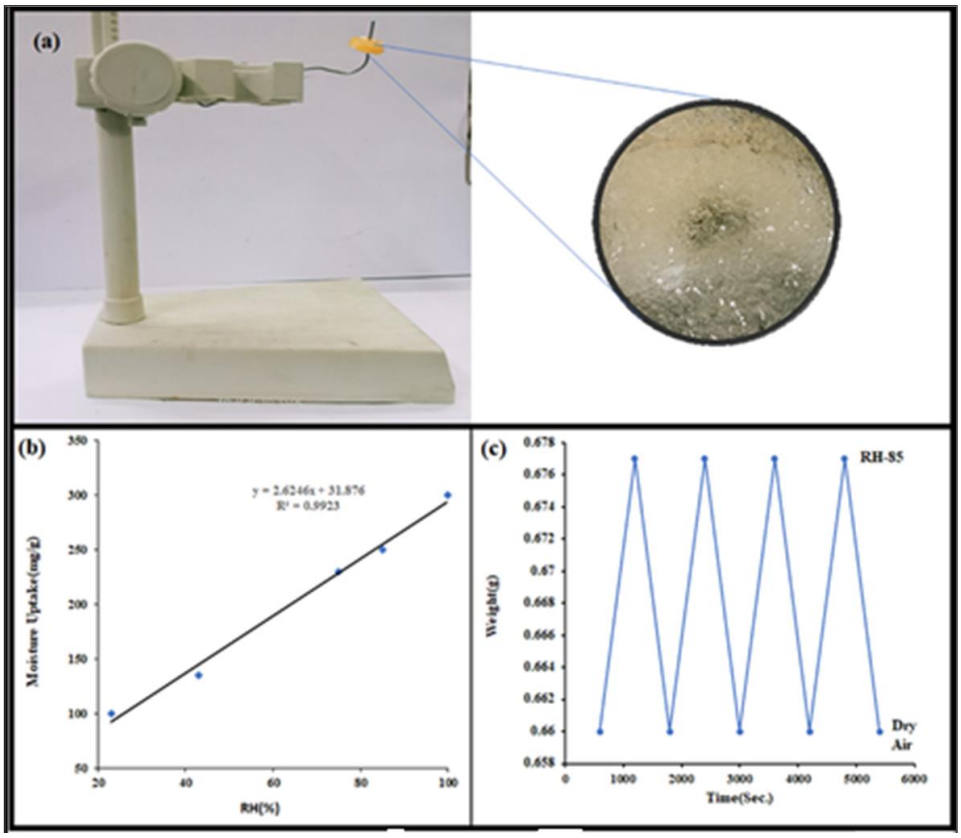

Fig. 9. (a) Optical photograph of GAHM, (b) Moisture uptake versus % RH plot for GAHM, (c) Drying-moisturizing cycles.

Finally, the calibration curve, shown in Fig. 9b was used to determine the % RH at various places, and the results were compared with the determination using the Air Humidity Meter PCE-EMD 5, PCE Instruments UK**.** A fair agreement was found between the % RH values determined by using GAHM and commercial instruments. The home town Jabalpur (our work place) (23.1815 o N,79.9864o E) was selected for the % RH measurement of air. The humidity of air was recorded at six different places using a mass measurement approach. The average % RH as determined by GAHM and Air Humidity Meter PCE-EMD 5 was 54.7±2.1 versus 56.1±1.9, respectively.

4. Conclusion

Because of H-bonding interactions and mutual entanglements within CMC and poly (AAm-co-VI) macromolecular chains, the solid hydrogel electrolyte (SHE) possesses self-healing, shape memory, adhesiveness, and flexibility. It also functions as a rechargeable supercapacitor, which lasts longer in the presence of glycerol. The hydrogel exhibits pH-

dependent swelling behavior, obtaining a higher degree of swelling at lower as well as higher pH. Furthermore, the presence of binary solvent (water + glycerol) and salt like $ZnCl_2$ in the hydrogel electrolyte renders it anti-freezing property to work in the range of -5 to 30 °C. Finally, sample SHE-I, used as GAHM, absorbs moisture in almost 600 s, and its calibration plot, obtained at various % RH, serves to determine the humidity in air, and the results are fairly accurate.

References

1. Z. Chen, J. Liu, Y. Chen, X. Zheng, H. Liu, and H. Li, ACS Appl. Mater. Interfaces **13**, 1353 (2020). https://doi.org/10.1021/acsami.0c16719
2. M. Hina, S. Bashir, K. Kamran, J. Iqbal, S. Ramesh, and K. Ramesh, Mater. Chem. Phys. **273**, ID 125125 (2021). https://doi.org/10.1016/j.matchemphys.2021.125125
3. S. Li, X. Zhou, Y. Dong, and J. Li, Macromol. Rapid Commun. **41**, ID 2000444 (2020). https://doi.org/10.1002/marc.202000444
4. 4. S. Li, Y. Cong, and J. Fu, J. Mater. Chem. B **9**, 4423 (2021). https://doi.org/10.1039/D1TB00523E
5. 5. Y. Wang, M. Zhu, X. Wei, J. Yu, Z. Li, and B. Ding, Chem. Eng. J. **425**, ID 130599 (2021). https://doi.org/10.1016/j.cej.2021.130599
6. H. Liu, T. Chen, C. Dong, and X. Pan, Hydrogels. **27**, 4647 (2020). https://doi.org/10.2174/0929867327666200408115817
7. E. Ahmadian, S. M. Dizaj, A. Eftekhari, E. Dalir, P. Vahedi, et al., Drug Res. **70**, 6 (2019). https://doi.org/10.1055/a-0991-7585
8. G. Chen, W. Tang, X. Wang, X. Zhao, C. Chen, and, Z. Zhu, Polymers **11**, ID 1420 (2019). https://doi.org/10.3390/polym11091420
9. H. Hong, Y. B. Seo, D. Y. Kim, J. S. Lee, Y. J. Lee, et al., Biomater. **232**, ID 119679 (2020). https://doi.org/10.1016/j.biomaterials.2019.119679
10. M. Askari, M. A. Naniz, M. Kouhi, A. Saberi, A. Zolfagharian, et al., Biomater. Sci. **9**, 535 (2021). https://doi.org/10.1039/D0BM00973C
11. H. Pangli, S. Vatanpour, S., Hortamani, R., Jalili, and A. Ghahary, J. Burn Care Res. **42**, 785 (2020). https://doi.org/10.1093/jbcr/iraa205
12. J. Amirian, Y. Zeng, M. I. Shekh, G. Sharma, F. J. Stadler et al., Carbohydr. Polym. **251**, ID 117005 (2020). https://doi.org/10.1016/j.carbpol.2020.117005
13. S. Qiang, D. Lijie, Z. Meifang, C. Xuetong, G. G. Hui, Mater. Chem. Phys. **193**, 57 (2017). https://doi.org/10.1016/j.matchemphys.2017.02.018
14. S. Y. Lee, S. I. Jeon, S. B. Sim, Y. Byun, and C.-H. Ahn, Acta Biomaterialia **131**, 286 (2021). https://doi.org/10.1016/j.actbio.2021.07.004
15. F. Chen, Y. He, Z. Li, Xu, B.Q. Ye *et al*. Int. J. Pharm. **606**, ID 120938 (2021). https://doi.org/10.1016/j.ijpharm.2021.120938
16. Y. Li, C. Liu, X. Lv, and S. sun, Soft Matter **17**, 2142 (2020). https://doi.org/10.1039/D0SM01998D
17. L. Debertrand, J. Zhao, C. Creton, and T. Narita, Gels **7**, 72 (2021). https://doi.org/10.3390/gels7020072
18. L. Hammer, N. J. Van Zee, and R. Nicolaÿ, Polymer **13**, ID 396 (2021). https://doi.org/10.3390/polym13030396
19. F. Ding, Y. Zou, S. Wu, and X. Zou, Polymer **206**, ID 122907 (2020). https://doi.org/10.1016/j.polymer.2020.122907
20. Y. -J. Wan, K. Rajavel, X. -M. Li, X. -Y. Wang, S.-Y. Liao, et al., Chem. Eng. J. ID 127303 (2020). https://doi.org/10.1016/j.cej.2020.127303
21. B. Fu, B. Cheng, X. Bao, Z. Wang, Y. Shangguan, and Q. Hu, J. Appl. Polym. Sci. **34**, ID 47885 (2019). https://doi.org/10.1002/app.47885

22. Y. Yan, J. Huang, X. Qiu, X. Cui, S. Xu et al., J. Colloid Interf. Sci. **582**, 187 (2021). https://doi.org/10.1016/j.jcis.2020.08.008
23. P. Suppakul, B. Chalernsook, , B. Ratisuthawat, S. Prapasitthi, and N. Munchukangwan, LWT Food Sci. Technol. **50**, 290 (2013). https://doi.org/10.1016/j.lwt.2012.05.013
24. S. Mali, M. V. E. Grossmann, M. A. García, M. N. Martino, and N. E. Zaritzky, J. Food Eng. **75**, 453 (2006). https://doi.org/10.1016/j.jfoodeng.2005.04.031
25. J. Tarique, S.M. Sapuan, and A. Khalina, Sci Rep. **11**, 13900 (2021). https://doi.org/10.1038/s41598-021-93094-y
26. X. Liu, Q. Zhang, Z. Gao, R. Hou, G. Gao, ACS Appl. Mater. Interf. **9**, 17645 (2017). https://doi.org/10.1021/acsami.7b04832
27. R. A. Talja, H. Helén, Y. H. Roos, and K. Jouppila, Carbohydr. Polym. **67**, 288 (2007). https://doi.org/10.1016/j.carbpol.2006.05.019
28. P. Suppakul, B. Chalernsook, B. Ratisuthawat, S. Prapasitthi, and N. Munchukangwan, LWT Food Sci. Technol. **50**, 290 (2013). https://doi.org/10.1016/j.lwt.2012.05.013
29. J. Tarique, S.M. Sapuan, and A. Khalina, Sci Rep. **11**, 13900 (2021). https://doi.org/10.1038/s41598-021-93094-y
30. P. Gajewski, W. Żyła, K. Kazimierczak, and A. Marcinkowska, Gels **9**, ID 527 (2023). https://doi.org/10.3390/gels9070527
31. N. M. Badawi, M. Bhatia, S. Ramesh, K. Ramesh, M. Kuniyil, et al., Polymers (Basel) **15**, ID 571 (2023). https://doi.org/10.3390/polym15030571
32. H. Xu, Q. Wang 1, Y. Deng, Z. Peng, and T. Wang, Electrochim. Acta **477**, ID 143785 (2024). https://doi.org/10.1016/j.electacta.2024.143785
33. M. G. Tadesse and J. F. Lübben, Gels **9**, 106 (2023). https://doi.org/10.3390/gels9020106
34. X. Wang, X. Wang, M. Pi, and R. Ran, Chem. Eng. J. **428**, ID 131172 (2022). https://doi.org/10.1016/j.cej.2021.131172
35. X. Sui, H. Guo, C. Cai, Q. Li, C. Wen et al., Chem. Eng. J. **419**, ID 129478 (2021). https://doi.org/10.1016/j.cej.2021.129478
36. P. He, R. Guo, K. Hu, K. Liu, S. Lin et al., Chem. Eng. J. **414**, ID 128726 (2021). https://doi.org/10.1016/j.cej.2021.128726